MOLECULAR ECOLOGY

Molecular Ecology (2009) **18**, 2877–2896 doi: 10.1111/j.1365-294X.2009.04245.x

Geographical variation in genetic structure of an Atlantic Coastal Forest frog reveals regional differences in habitat stability

SARAH W. FITZPATRICK,* CINTHIA A. BRASILEIRO,† CÉLIO F. B. HADDAD† and KELLY R. ZAMUDIO*

Department of Ecology and Evolutionary Biology, Cornell University, E145 Corson Hall, Ithaca, NY 14853, USA, †Departamento de Zoologia, Instituto de Biociências, Universidade Estadual Paulista, Caixa Postal 199, 13506-900 Rio Claro, SP, Brazil

Abstract

Climatic oscillations throughout the Pleistocene combined with geological and topographic complexity resulted in extreme habitat heterogeneity along the Atlantic coast of Brazil. Inferring how these historic landscape patterns have structured the current diversity of the region's biota is important both for our understanding of the factors promoting diversification, as well as the conservation of this biodiversity hotspot. Here we evaluate potential historical scenarios of diversification in the Atlantic Coastal Forest of Brazil by investigating the population genetic structure of a frog endemic to the region. Using mitochondrial and nuclear sequences, we generated a Bayesian population-level phylogeny of the *Thoropa miliaris* species complex. We found deep genetic divergences among five geographically distinct clades. Southern clades were monophyletic and nested within paraphyletic northern clades. Analyses of historical demographic patterns suggest an overall north to south population expansion, likely associated with regional differences in habitat stability during the Pliocene and early Pleistocene. However, genetic structure among southern populations is less pronounced and likely represents more recent vicariant events resulting from Holocenic sea-level oscillations. Our analyses corroborate that the Atlantic Coastal Forest has been a biogeographically dynamic landscape and suggest that the high diversity of its fauna and flora resulted from a combination of climatic and geologic events from the Pliocene to the present.

Keywords: glacial refugia, mitochondrial DNA, phylogeography, population expansion, *Thoropa miliaris*, *Thoropa taophora*

Received 15 July 2008; revision received 20 March 2009; accepted 13 April 2009

Introduction

The Atlantic Coastal Forest of Brazil is ranked among the top five biomes in priority for biodiversity conservation, primarily owing to its high levels of endemism, species richness, and high rates of habitat loss (Brown & Brown 1992; Morellato & Haddad 2000; Myers *et al*. 2000). Compared to other South American biomes, this region has the highest species diversity for its size; its degree of endemism, as high as 90% in some groups and averaging 50% overall, is surpassed only by the Amazon (Costa *et al*. 2000). The Atlantic Coastal Forest has experienced dramatic habitat modification and fragmentation and remains under severe anthropogenic pressure, with only 7.3% of primary forest currently intact (Morellato & Haddad 2000). Despite these dramatic losses, researchers continue to discover new species, diverse plant–animal interactions, and novel features of natural history (Costa *et al*. 2000; Morellato & Haddad 2000; Pizo & Oliveira 2000; Haddad & Prado 2005; Brasileiro *et al*. 2007a, b, c). However, only a few studies of this megadiverse biome have addressed the evolutionary origins of its biodiversity (Moritz *et al*. 2000; Carnaval 2002; Pellegrino *et al*. 2005; Grazziotin *et al*. 2006; Cabanne *et al*. 2007; Carnaval & Bates 2007; Carnaval *et al*. 2009).

Correspondence: Sarah W. Fitzpatrick, Fax: (607) 255-8088; E-mail: sf83@cornell.edu

The Atlantic Coastal Forest occupies the eastern edge of the Brazilian shield where it drops off as an escarpment towards the sea (Martins & Coutinho 1981). The coastline is topographically complex over short geographical distances, having been shaped by tectonic activity in the Tertiary and by glacially driven sea-level changes in the Quaternary (Suguio & Martin 1978; Caruso *et al*. 2000; Suguio 2004; Souza *et al*. 2005). One hypothesis for Atlantic Coastal Forest diversification posits that the uplift of the east coast of Brazil in the Tertiary resulted in geographical and climatic modifications, leading to forest fragmentation, isolation of regional faunas, and correlated speciation events (Simpson 1979). A second hypothesis posits that more recent Pleistocene glacial cycles have resulted in vicariance of populations in refuges along the coast (Haffer 1969; Grazziotin *et al*. 2006; Carnaval & Bates 2007) as well as the isolation of populations on continental islands due to climate-induced sea-level changes (Marques *et al*. 2002; Grazziotin *et al*. 2006; Brasileiro *et al*. 2007a, b, c). Pleistocene glacial cycles resulted in several dry climatic periods during the Quaternary causing alternating cycles of contracting and expanding tropical forest patches. Repeated periods of isolation may have contributed to diversification of species adapted to both forests, savanna habitats, and other open formations (Haffer 1969; Vanzolini & Williams 1981; Haffer & Prance 2001). Although this hypothesis has been tested primarily in Amazonia, more recent studies indicate that cyclical climate changes also had significant effects on the fragmentation and persistence of forested regions within Atlantic Coastal Forest (Carnaval & Bates 2007), and in fact, palynological studies suggest that large open areas dominated the Atlantic Forest during the Late Pleistocene and that patches of forest were widely isolated (Ledru *et al*. 1998; Behling & Negrelle 2001). Most empirical studies of Brazilian taxa to date have focused on differentiation during the Pleistocene (Lara & Patton 2000; Glor *et al*. 2001; Ribas & Miyaki 2004; Wüster *et al*. 2005); however, recent surveys of the timing of diversification for Neotropical lineages indicates that diversification trends have been continuous, without significant differences between Tertiary and Quaternary speciation rates (Zink *et al*. 2004; Rull 2008).

Recent paleoclimatic modelling of predicted habitat stability in the Atlantic Forest corroborates the hypothesis that the distribution of forested habitat was spatially and temporally variable during Late Pleistocene glaciations (Carnaval & Moritz 2008). Those climatic changes in combination with the geomorphologic complexity of this coastline could result in fine-scale habitat heterogeneity, potentially magnifying highly regionalized and variable responses to climate, and increasing diversity and endemism in the Atlantic Forest (Suguio & Martin 1978; Carnaval & Moritz 2008). The paleoclimatic model uncovered striking regional differences in the persistence of paleorefuges throughout the Quaternary, with a sharp contrast between historically stable regions of forested habitats in the northernmost regions of the Atlantic Forest and an apparent lack of potential refuges in the south. If this model is correct, the genetic signature of populations in the north should differ in a predictable fashion from those further south. Specifically, we would predict relatively high genetic diversity in northern populations and signatures of more recent population expansion as southern regions became secondarily colonized.

Published phylogeographical data provide mixed support for the habitat stability model (Carnaval & Moritz 2008). Some taxa demonstrate the predicted higher genetic diversity in northern regions and evidence of late Quaternary population expansion in the south (Pellegrino *et al*. 2005; Grazziotin *et al*. 2006; Cabanne *et al*. 2007; Carnaval *et al*. 2009), but other taxa show idiosyncratic patterns throughout all regions of Atlantic Coastal Forest (Costa 2003; Leite 2003). In addition, the model of Carnaval & Moritz (2008) does not account for the high incidence of endemism in taxa occurring primarily in southern forests (Costa *et al*. 2000; da Silva *et al*. 2004; Pinto-da-Rocha & da Silva 2005), suggesting that a single model of diversification within this biome is not realistic. However, detailed phylogeograph studies of Atlantic Forest organisms are few in number and taxonomic coverage (Costa 2003; Leite 2003; Pellegrino *et al*. 2005; Grazziotin *et al*. 2006; Cabanne *et al*. 2007). The poor predictive performance of the Carnaval & Moritz (2008) model in the southeastern regions of the Atlantic forest emphasizes the need for phylogeograph studies that focus on taxa with broader distributions in the southernmost regions.

In this study, we reconstruct the phylogeography of the *Thoropa miliaris* species complex, a frog endemic to the Atlantic Coastal Forest. Anurans are particularly appropriate for investigations involving hypotheses about habitat stability because they are highly sensitive to climatic changes owing to complex life cycles, permeable skin, and exposed eggs (Carey & Alexander 2003). The *T. miliaris* species complex is comprised of two polytypic congeners, *T. miliaris* and *T. taophora* (Feio *et al*. 2006). The two species in this complex were recently recognized based on geographical morphological variation (Feio *et al*. 2006); however, the genetic diversity of the species complex has not been previously studied. *Thoropa miliaris* has a more northern distribution in the Brazilian states of Espírito Santo and Rio de Janeiro, while *T. taophora* is restricted to the southern state of São Paulo (Fig. 1; Feio *et al*. 2006). Both species are characterized by male egg attendance, high levels of territoriality, and habitat specialization with semi-terrestrial tadpoles living on humid rocky walls (Giaretta & Facure 2004). They occur on rocky substrates along the Brazilian coast, inhabiting seeps and small freshwater streams as well as rocky marine shores between the elevations of 0–1100 m (Bokermann 1965; Sazima 1971). The southern

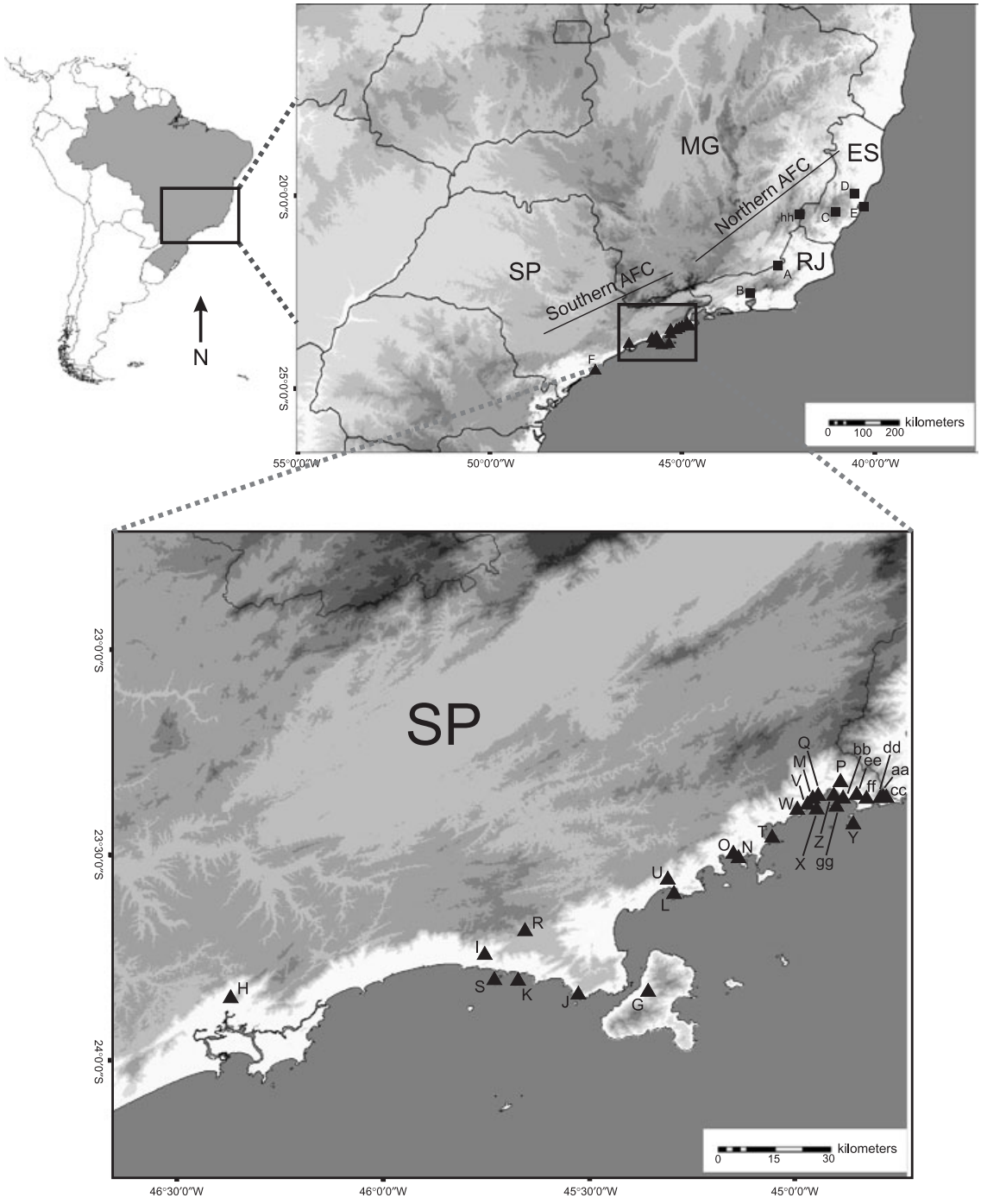

Fig. 1 Sampling localities for individuals of *Thoropa miliaris* and *T. taophora* included in this study. Letters correspond to locality names in Appendix. Squares and triangles represent *T. miliaris* samples from northern regions and *T. taophora* from southern regions of Atlantic Coastal Forest, respectively.

populations of *T. taophora* have high salinity tolerance, often feeding on marine invertebrates in the intertidal zone, a niche that is rarely occupied by amphibians (Sazima 1971; Abe & Bicudo 1991; Siqueira *et al*. 2006). These natural history characteristics possibly facilitated the persistence of several populations on continental islands off the São Paulo coastline, providing an opportunity to test hypotheses about the historical effects of climate and topography on differentiation of mainland and island populations of a single Atlantic Coastal Forest taxon.

We quantified genetic variability of populations throughout the range of the *T. miliaris* species complex. We used

Table 1 Primers used for amplification and sequencing of mitochondrial and nuclear genes in *Thoropa miliaris* and *Thoropa taophora*

Primer	Fragments	Sequence (5′–3′)	Source
tmFibRl	β-fibrinogen	TTCACAATGGCATGTTCTTCA	This study
tmFibFl	β-fibrinogen	CCAGTAGTATCTGCCATTAGGGTTA	This study
Fib-B17U	β-fibrinogen	GGAGAAAACAGGACAATGACAATTCAC	Prychitko and Moore (1997)
Fib-17L	β-fibrinogen	TCCCCAGTAGTATCTGCCATTAGGGTT	Prychitko and Moore (1997)
L4437	ND2	AAGCTTTCGGGCCCATACC	Macey *et al.* (1997)
H5934	ND2	ARGGTGCCAATGTCTTTGTGRTT	Macey *et al.* (1997)
CytbA-L	control	GAATYGGRGGWCAACCAGTAGAAGACCC	Goebel *et al.* (1999)
Control P-H	control	GTCCATAGATTCASTTCCGTCAG	Goebel *et al.* (1999)
16SB-H	16S	CCCGTCTGAACTCAGATCACGT	Vences *et al.* (2000)
16SA-L	16S	CGCCTGTTTATCAAAAACAT	Vences *et al.* (2000)

mitochondrial and nuclear markers to test hypotheses about the evolutionary history of this endemic frog and possible scenarios to explain the origins of Atlantic Coastal Forest diversity. Specifically, our goals were to (i) assess the regional population structure and distribution of genetic variability within the *T. miliaris* species complex; (ii) determine geographical barriers to gene flow and timing of divergences among mainland populations; and (iii) evaluate whether signals of historical isolation and expansion are compatible with previous hypotheses of the origins of Atlantic Coastal Forest diversity. Our study contributes to the understanding of the role that historical climatic fluctuations have played in the origin and maintenance of diversity and endemism in this poorly known and highly endangered biome.

Materials and methods

Sample collection and molecular methods

We collected samples of the *Thoropa miliaris* species complex from throughout its distribution in the Atlantic Forest of Brazil during the years of 2004–2007. We sampled a total of 137 individuals from 34 populations with a range of 1–10 individuals per site (Fig. 1; Appendix). The sampling localities span the species' distribution from southern São Paulo to northern Espírito Santo. We also included nine populations from islands off the southeastern coast of São Paulo. We collected *Thoropa megatympanum*, and *Cycloramphus dubius* as successively distant outgroup species for our phylogeograph analysis (Frost *et al.* 2006).

Tissues were sampled as toe clips, liver samples, or tadpoles, and preserved in 95% ethanol before DNA extraction. We extracted total cellular DNA with DNeasy Tissue kits using manufacturer's protocols (QIAGEN). We eluted DNA extracts in 200 μL buffer for use as template in polymerase chain reaction (PCR) amplifications. We amplified and sequenced three mitochondrial gene regions: (i) the control region and a short segment of the adjacent cytochrome *b* gene (referred to as the control region, 932 bp), (ii) part of the 16S gene (622 bp), and (iii) the complete NADH dehydrogenase subunit 2 and the five adjacent tRNAs (WANCY: $tRNA^{trp}$, $tRNA^{ala}$, $tRNA^{asn}$, $tRNA^{cys}$, $tRNA^{tyr}$). For simplicity, we refer to this third segment as the ND2 fragment (1424 bp). In addition, we sequenced one nuclear intron, β-fibrinogen (619 bp), for 129 individuals. Amplification and sequencing primers are listed in Table 1. Amplifications were performed in 25-μL reaction volumes each containing 100 ng DNA template, 1 × reaction buffer with 1.5 mM $MgCl_2$, 0.76 mM dNTPs, 0.4 mM of each primer (forward and reverse) and 0.625 U *Taq* buffer. PCR conditions consisted of 5-min initial denaturation at 94 °C, 35 amplification cycles of 1-min denaturation at 94 °C, 1-min annealing at fragment-specific temperature, 1-min extension at 72 °C, and a final 5-min extention at 72 °C. Annealing temperatures for gene fragments were 55.8 °C for ND2, 57.6 °C for 16S and the control region, and 45 °C for β-fibrinogen. We electrophoresed the resulting PCR products on a 2% agarose gel and visualized products with ethidium bromide staining to verify their size. Successful amplicons were purified with shrimp alkaline phosphatase (1 U) and exonuclease I (10 U) to remove dNTPs and primer pairs. All regions were sequenced in both directions using the original amplification primers and BigDye termination sequencing chemistry. Sequencing reactions were carried out in a total volume of 5 μL with 1 μL cleaned PCR product, 0.12 μL of 10 μM primer, 1 μL Ready Reaction Mix, and 0.5 μL Sequencing Buffer (Applied Biosystems). Cycle sequencing products were purified with Sephadex G-50 and eletrophoresed on an ABI PRISM 3700 DNA Analyser.

Alignment and phylogenetic analyses

We checked electropherograms by eye before constructing contiguous sequences for each fragment using Sequencher version 4.7 (Gene Codes). Each gene was aligned separately using ClustalW (Thompson *et al.* 1994) in the MEGALIGN version 6.1.2 program of the Lasergene sequence analysis software (DNASTAR). To identify regions of ambiguous homology, we performed independent alignments using

four different gap penalties: (5, 10, 15, 20) for the ND2 and 16S sequences and (10, 15, 20, 25) for the control region sequences (Gatesy *et al*. 1993). Gap length was held constant (0.2) for each gene. All other parameters were set to default settings. We excluded from phylogenetic analyses all sites that varied in alignment across these ranges of parameters.

The best-fit model of evolution for each gene partition was estimated using ModelTest version 3.7 (Posada & Crandall 1998), and selected based on the Akaike information criterion (AIC). We concatenated all mitochondrial sequences to determine haplotypes for each individual and used PAUP* version 4.0b10 (Swofford 2002) to determine unique haplotypes [across all three mitochondrial DNA (mtDNA) genes] in our data set. We inferred a population-level phylogeny using fully partitioned Bayesian Inference (BI) implemented in MrBayes 3.0b4 (Huelsenbeck & Ronquist 2001). The Bayesian analysis consisted of two independent runs each of 10 chains sampling every 1000 generations for 20 million generations to assure independence of the samples. We used two methods to verify convergence and determine adequate burn-in. First, we examined a plot of likelihood scores of the heated chain. Second, we checked the stationarity of chains using the software Tracer version 1.4 (Rambaut & Drummond 2004). We disregarded a total of 5000 trees as burn-in; using the remaining trees, we estimated the 50% majority-rule consensus topology with branch lengths and posterior probabilities for each node in MrBayes.

To compare patterns of divergence in β-fibrinogen and mtDNA data sets, we used the program Phase version 2.02 (Stephens *et al*. 2001; Stephens & Donnelly 2003) to determine independent nuclear alleles for all individuals that were polymorphic for more than one segregating site. We ran Phase under default conditions, including 100 iterations, 10 iterations discarded as burn-in, and a thinning interval of 1. We ran the algorithm three times with different random number seeds and recovered the same haplotypes each time. We removed poorly resolved haplotypes (< 0.9) from subsequent analyses and used remaining nuclear alleles to construct a minimum-spanning network in TCS version 1.21 (Clement *et al*. 2000). We used a 95% parsimony connection threshold and disregarded ambiguities among sequences that resulted from missing data. Our decision to use statistical parsimony (Templeton *et al*. 1992) to examine evolutionary relationships among nuclear sequences was based on overall lower levels of nucleotide diversity and the fact that we obtained nuclear sequences for a subset of individuals included in the mtDNA sample (Appendix).

Mitochondrial DNA diversity indices and population differentiation

The Bayesian topology revealed well-supported clades corresponding to distinct geographical regions. Haplotype diversity (*h*) and nucleotide diversity (Tajima 1983; Nei 1987) were estimated using Arlequin 3.01 (Schneider *et al*. 2000). We estimated overall genetic differentiation between pairs of population samples with pairwise fixation indices (F_{ST}) that were tested for significance by comparison to a simulated null distribution of no difference among the populations using 10 000 random permutations in Arlequin.

To explore the population structure of *T. miliaris* and *T. taophora* without making a priori assumptions about partitions of local populations, we used a spatial analysis of molecular variance implemented in the program SAMOVA version 10 (Dupanloup *et al*. 2002). This method is based on Φ-statistics and uses a simulated annealing procedure, with 100 initial conditions, to define groups of populations that are geographically homogeneous and maximally differentiated from each other. We tested population partitions ranging from 2 to 11 to examine the proportion of genetic variance due to differences among groups (F_{CT}) and find the range of K for which F_{CT} was largest and statistically significant. The overall genetic variation was then partitioned into its hierarchical components among groups, among populations within groups, and within populations using an analysis of molecular variance (AMOVA; Excoffier *et al*. 1992) as implemented in the Arlequin software (Schneider *et al*. 2000). This analysis was based on pairwise squared-Euclidean distances between haplotypes with 10 000 permutations and the Tamura molecular distance estimates to allow unequal rates of transition and transversion (Tamura 1992).

Timing of divergences

For each node of interest, time to most recent common ancestor (TMRCA) for clade haplotypes were obtained using the Bayesian Markov Monte Carlo method implemented in BEAST version 1.4.7 (Drummond *et al*. 2002; Drummond & Rambaut 2007). We lacked a fossil calibration for any frog in this family and given the variance in mutation rates among vertebrate mtDNA loci (Brown *et al*. 1982), we used the best available independent estimate of mutation rate for the genes we sequenced. We performed our final analyses using only our ND2 sequences and a mutation rate derived from the leptodactylid frog *Craugastor* (0.957% per lineage per million years; Crawford 2003). We performed two parallel analyses, the first including sequences from all populations, and the second excluding all island populations, to ascertain that isolated island populations did not inflate our time estimates. We also implemented a series of coalescent models (Bayesian skyline, exponential, expansion) to assess any bias these models might have on time estimates. For each analysis, we performed two independent runs of 10–25 million generations sampling every 1000th generation and removing 10% of the initial samples as burn-in. We combined the runs and determined stationarity

of the posterior distributions for all model parameters using Tracer 1.4 (Drummond & Rambaut 2007). We implemented a relaxed molecular clock with uncorrelated rates among lineages, and the following substitution model priors: rate parameters uniform (0,500); alpha exponential (1); proportion of invariant sites uniform (0,1). Scale operators were adjusted as suggested by the program.

Historical demographic patterns

We tested our hypotheses about demographic stability in different parts of this species' range by using the mtDNA sequences in a mismatch distribution test of genetic differences between pairs of haplotypes (Rogers & Harpending 1992). This analysis distinguishes among populations that have undergone rapid population expansions from those that have a history of long-term demographic stability. Populations in demographic equilibrium have multimodal mismatch distributions, whereas a smooth unimodal distribution suggests a recent demographic expansion (Rogers & Harpending 1992). To test the hypothesis of regional differences in historical habitat stability, we tested whether northern populations (from the Rio de Janeiro and Espírito Santo sites) showed a pattern of demographic stability and whether the data showed a genetic signature of north to south expansion.

We conducted the mismatch distribution test using Arlequin 3.01 to test for demographic expansion in regional groups of populations uncovered by phylogenetic analysis (Table 4). These analyses tested for demographic expansion in three of the five regional clades distinguished by phylogenetic analysis (North 2, São Paulo south, São Paulo north); we excluded the groups North 1 and Juréia due to inadequate sample sizes for mismatch distributions. The fit of mismatch distributions to the expansion model was assessed with 100 bootstrap replicates. For clades showing evidence of expansion, we compared the sum of square deviations (SSD) between the observed and the expected mismatch to test our hypothesis of a stepwise north to south expansion model (Schneider & Excoffier 1999); a significant P value rejects the fit of the data to the expansion model. Additionally, tests of selective neutrality were performed using Tajima 1989 and Fu 1997 test statistics where historical population growth predicts significantly negative D and F_S values. The significance of deviation from values expected under demographic stationarity was tested with 10 000 bootstrap replicates.

Mismatch distributions and neutrality tests fail to make full use of historical signal within DNA sequences as they are based solely on the number of segregating sites and the distribution of haplotypes. To reconstruct changes in demographic growth over the history of each major lineage, we used the coalescent-based method of Bayesian skyline plots (BSP, Drummond *et al*. 2005). This approach allows inferences of population fluctuations over time by estimating the posterior distribution for effective population size at intervals along a phylogeny. We used concatenated mtDNA sequences for this analysis and fixed the mean substitution rate at 1.0 so as to estimate time in units of substitution/site. We used the default settings for skyline model (linear) and number of groups (10). Analyses were run for 15 million steps, sampling every 1000 steps, and discarding 1000 samples as burn-in. We repeated analyses twice with different random seeds to test for convergence, combined results from multiple runs, and visualized skyline plots using Tracer 1.4 (Rambaut & Drummond 2004).

Results

Alignment and phylogenetic analyses

The final alignment of the three mtDNA gene fragments included 622 bp for 16S, 1424 for ND2, and 930 bp for the control region. We excluded 340 bp (57 bp in 16S; 63 bp in ND2; 220 bp in the control region) due to ambiguous homology. All ambiguities in alignment for the ND2 gene fragment were present in the five tRNAs adjacent to the coding region. In the final data set, 847 bp were variable and 608 were parsimony informative. We obtained sequences for 137 individuals from 33 sampling localities and identified 105 unique haplotypes (for the three mtDNA genes combined). Duplicate haplotypes only occurred among individuals collected from the same site (Appendix). The diversity of mitochondrial haplotypes within populations differed across the range. In northern localities, all individuals sampled had a unique haplotype; in contrast, among southern localities we recovered 85 haplotypes from 116 individuals sampled.

Hierarchical tests for the model of nucleotide evolution showed that the model TIM + G (Rodriguez *et al*. 1990), TrN + I + G, and HKY + G (Hasegawa *et al*. 1985) best fit the control region, 16S, and ND2 data, respectively. We inferred a phylogenetic tree using a fully partitioned Bayesian analysis of all unique haplotypes. The Bayesian consensus tree (Fig. 2) supported the monophyly of the *Thoropa miliaris* species complex relative to the two outgroups. The main pattern evident in our ingroup is the hierarchical nesting of recently diverged southern haplotype clades within paraphyletic northern clades. The large clade including populations in São Paulo state, includes a well-supported basal separation between haplotypes from the single southern locality Juréia and all remaining São Paulo localities. Most haplotypes collected in the northern or southern localities from São Paulo state belong to geographically concordant clades (São Paulo north or São Paulo south). We found no haplotypes from individuals collected south of Praia Domingas Dias (O) in the northern

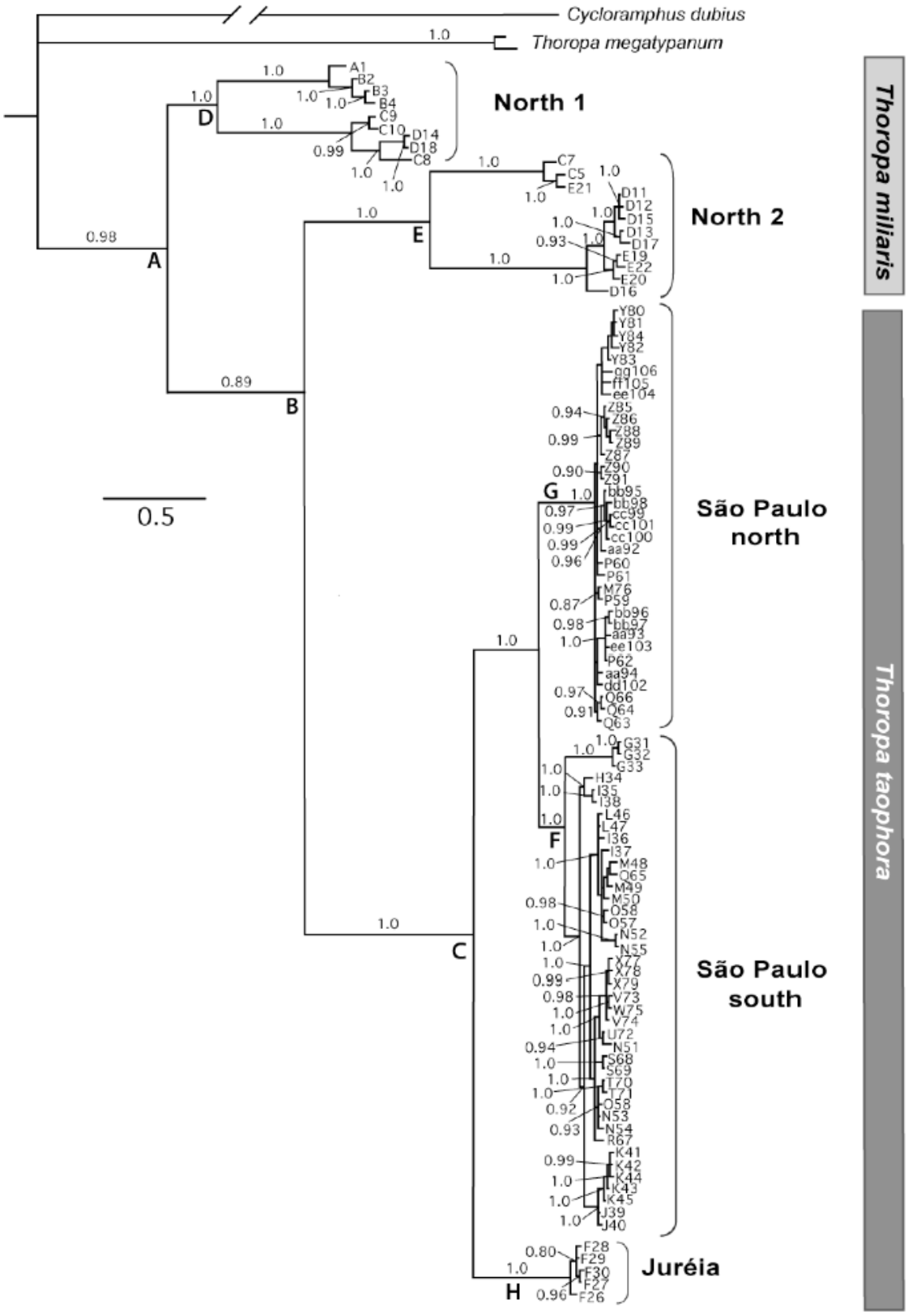

Fig. 2 Bayesian tree topology inferred from three mtDNA gene fragments (control region, 16S, and ND2) for the *Thoropa miliaris* species complex. Letters and numbers at branch tips correspond to localities and haplotype numbers sampled throughout the Atlantic Coastal Forest of Brazil (Appendix). Posterior probabilites > 70% are indicated by numbers above branches.

Table 2 Genetic diversity indices for mitochondrial haplotypes from five clades of the *Thoropa miliaris* species complex. Nuclear diversity indices were estimated for all populations combined

	No. of samples	No. of haplotypes	No. of observed nucleotide sites	No. of polymorphic sites	Mean no. of pairwise differences	Nucleotide diversity (π)	Haplotype diversity (h)
mtDNA							
North 1	9	9	2484	195	94.00 ± 44.73	0.038 ± 0.020	1.00 ± 0.052
North 2	12	12	2504	183	71.9 ± 33.38	0.029 ± 0.015	1.00 ± 0.034
Juréia	6	5	2510	9	4.2 ± 2.43	0.0017 ± 0.0011	0.933 ± 0.122
São Paulo south	59	40	2560	110	16.37 ± 7.40	0.0064 ± 0.0032	0.983 ± 0.006
São Paulo north	46	35	2565	55	7.44 ± 3.54	0.0029 ± 0.0015	0.984 ± 0.009
nuclear							
combined	129	18	509	45	4.213 ± 2.106	0.0083 ± 0.005	0.847 ± 0.021

São Paulo clade. However, the southern São Paulo clade contains several haplotypes from northern São Paulo localities.

We sampled nine populations from continental islands that have only recently been isolated from coastal populations due to sea level oscillations during the late Pleistocene and Holocene (Suguio & Martin 1978). Despite the recency of isolation, individuals from islands were often more closely related to each other than to any other population. We found different levels of genetic structure among island haplotypes in our southernmost clades. Haplotypes from Ilha de São Sebastião (G), Ilha Prumirim (X), Ilha de Toque Toque (J) and Ilha dos Gatos (K) each form a well-supported monophyletic group nested within São Paulo south. In contrast, the island haplotypes from within the northern São Paulo [Ilha Redonda (Z), Ilha de Porcos Pequena(gg), Ilha das Couves Norte(Y)] do not form well-supported clades, but rather are admixed among the poorly structured haplotypes of the São Paulo north clade. Finally, samples from Juréia, a coastal locality that was isolated as an island 5000 years ago (Marques & Duleba 2004) forms a clade that diverged early from all other São Paulo populations.

We removed nine individuals from the nuclear data set due to unresolved haplotypes in the Phase runs. The excluded individuals were duplicates, therefore all sampled populations were represented in final data set. The β-fibrinogen gene fragment showed lower overall diversity with only 45 polymorphic sites in the 619 bp sequenced and only 39 unique sequences among the 240 inferred haplotypes. Despite lower levels of diversity and lower mutation rates in our nuclear marker, the minimum-spanning network depicted patterns of geographical genetic distribution similar to those recovered in our mitochondrial phylogeny (Fig. 3). All individuals sampled from the northern region showed significant differentiation; the northern group included 10 individuals represented by 11 haplotypes that were significantly differentiated and did not connect to the southern alleles at the 95% parsimony threshold. Twenty-four mutational steps were required to connect all northern alleles to the network. In contrast, the network revealed considerable admixture among São Paulo populations. Haplotypes differed by no more than two mutational steps and the most frequent haplotype from São Paulo was found in 37 individuals from 16 populations. The network also corroborates the differentiation of samples from Juréia from all other São Paulo populations.

Mitochondrial DNA diversity indices and population differentiation

We estimated haplotype and nucleotide diversity for each main clade identified in the phylogenetic analysis (Table 2). Nucleotide diversity (π) varied regionally by an order of magnitude. Northern groups showed the highest nucleotide diversity ranging from 0.029–0.038 whereas the São Paulo clades and Juréia ranged from 0.0017–0.0064 reflecting high sequence similarity. All groups had high haplotypic diversity, particularly in the north where every haplotype was unique ($h = 1.00$). Haplotypic diversity of São Paulo groups and Juréia were also high, ranging from 0.933–0.984 (Table 2).

Pairwise population estimates of F_{ST} based on the mitochondrial data for the 33 localities revealed a wide range of interpopulation genetic differentiation (Table S1, Supporting information). Significant F_{ST} values ranged from 0.06 (BR101 wall km 16.9–Domingos Martins) to 0.78 (Ilha de Porcos Pequena–Ilha Couves Sul). Population pairs with high and significant F_{ST} values were consistently found between distant or isolated localities. Island populations such as Porcos Pequena yielded the highest significant pairwise F_{ST} values as expected due to their isolation.

Results of the SAMOVA analyses showed rising values of F_{CT} and decreasing F_{SC} as the number of population groupings (K) increased. However, the sequential analyses with values of K ranging from two-11 showed that highest

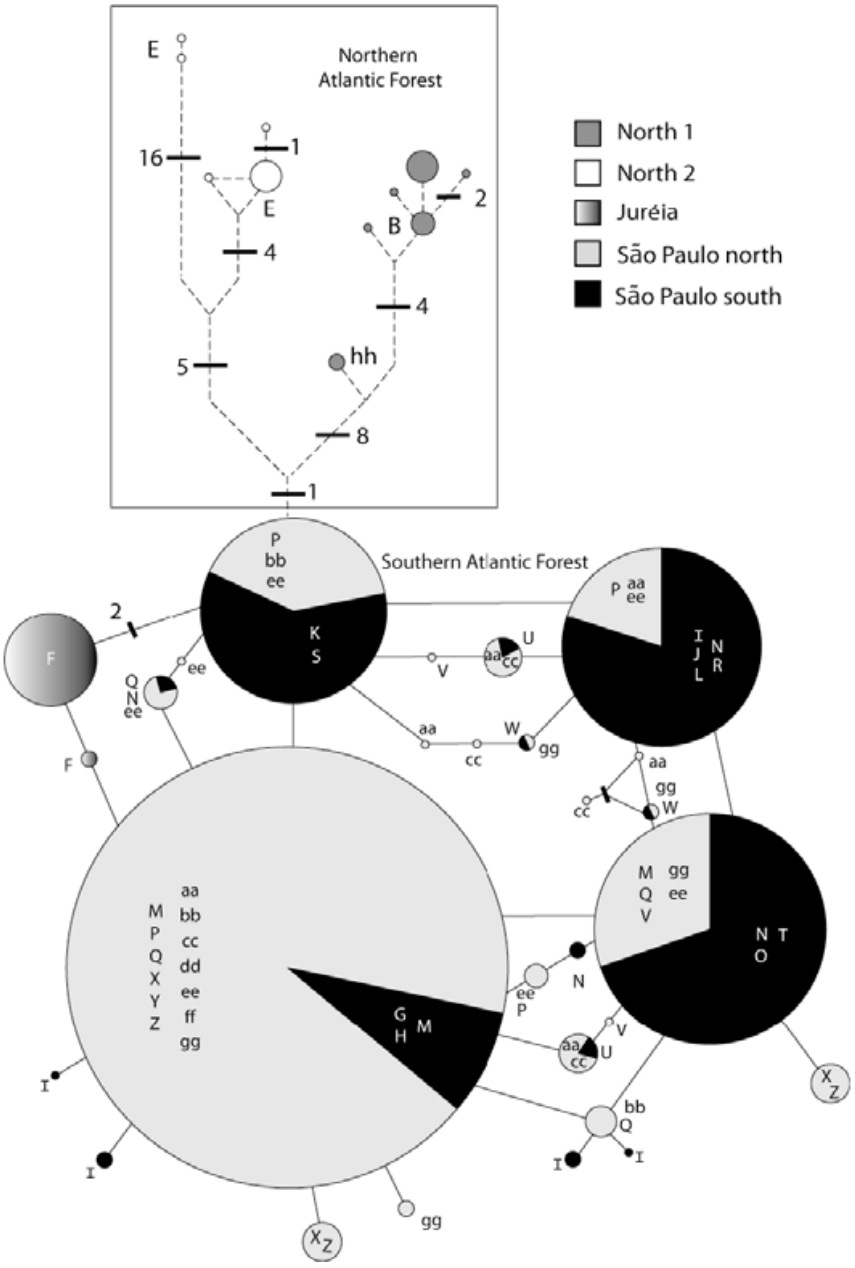

Fig. 3 Unrooted 95% parsimony network based on 619 bp of nuclear DNA sequence (β-fibrinogen) for 240 haplotypes of *Thoropa miliaris* and *T. taophora*. Shared haplotypes are indicated by circles with area proportional to the number of individuals contained within; letters correspond to populations represented within the circle. Solid and dashed lines represent parsimonious connections between haplotypes corresponding to a single point mutation. Numbers and hyphens indicate number of mutational steps between haplotypes. Colours and patterns represent the five geographical clades inferred from Bayesian analysis. Nuclear sequences of individuals from the two northern clades are included in the outlined box.

among group variation (F_{CT} = 0.780) occurred for nine groups [(D); (E); (C); (F); (U); (G); (B, A); (K, J); (H, gg, L, I, X, Z, S, Y, T, M, V, W, O, bb, N, ff, cc, aa, dd, ee, Q, P)]. Hierarchical analyses of concatenated sequences revealed significant variation among groups and within populations (AMOVA; Table 3) indicating high levels of geographical structuring and restricted gene flow. Genetic differences among groups explained 70% of the variance (Φ_{CT} = 0.703). In contrast, 16% of the total genetic variance was explained by differences among populations within groups (Φ_{SC} = 0.540), and 14% of the variance was attributed to genetic differences within populations (Φ_{ST} = 0.863).

Timing of divergences

The estimates of TMRCA (for the haplotype clades of interest (Fig. 2) were highly concordant among runs (Table 5), independent of the coalescent model applied, and inclusion of island populations. The estimated TMRCA for the basal node (Node A) was 9–12 million years ago over all coalescent models. The oldest cladogenic divergences between northern clades occurred in the Pliocene or Miocene (Node B; 8.1–8.9 million years ago) whereas the southern populations show more recent divergences in the Pleistocene or late Pliocene (Node C; 3.1–3.4 million

Table 3 Results of the analysis of molecular variance (AMOVA) for genetic divergences in mtDNA sequence data. Populations were partitioned into nine groupings as inferred by SAMOVA. The percentages of total variance explained for each grouping, fixation indices, and their significance based on 10 000 random permutations are included for each hierarchical level. Significant *P* values are bolded

Source of variation	d.f.	Percentage of total variance	Fixation indices	*P* value
Among groups	8	70.28	$\Phi_{CT} = 0.703$	**< 0.0001**
Among populations within groups	23	16.06	$\Phi_{SC} = 0.540$	**< 0.0001**
Within populations	100	13.67	$\Phi_{ST} = 0.863$	**< 0.0001**
Total	131			

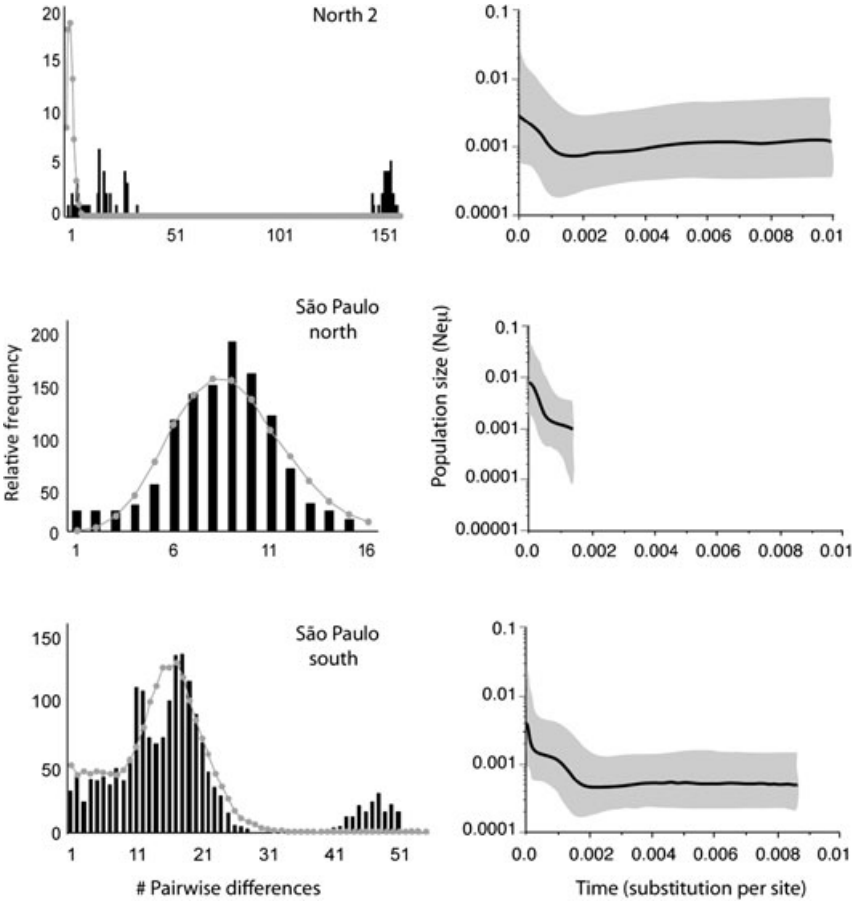

Fig. 4 Historical demographic history of *Thoropa miliaris* and *T. taophora* inferred from ND2 mitochondrial DNA sequences. (a) Pairwise mismatch distributions for three geographical regions uncovered in our phylogenetic analysis. Black columns represent the observed frequencies of pairwise differences among haplotypes. Gray lines and circles show the expected values for populations that have undergone historical demographic expansion. (b) Bayesian skyline plots for the same regional groups, showing effective population size as a function of time. Black lines represent median population estimates and gray lines denote upper and lower confidence limits (95% HPD).

years ago). Within southern groups, the diversification of populations in the São Paulo south lineage (Node F; 0.5–1.1 million years ago) predated that of São Paulo north populations (Node G; 0.2–0.3 million years ago), and haplotypes from Juréia diversified most recently (Node H; 0.2 million years ago).

Historical demographic patterns

Plots of mismatch distributions revealed differences in demographic stability between northern and southern regions (Fig. 4). The observed haplotype mismatch distributions for clade North 2 was multimodal, a signature of historic demographic stability. Mismatch analyses for São Paulo north and south haplotypes revealed unimodal distributions that conform to the null model of expansion (Table 4). Tajima's *D* and Fu's *F* were calculated as additional tests for expansion based on deviation from neutrality and corroborated the evidence for expansion in southern regions. Fu's *F* yielded significantly negative values for both São Paulo clades and Tajima's *D* was significantly negative for São Paulo north (Table 4).

Bayesian skyline plots (BSP) depict the demographic history of the same three clades analysed by mismatch tests (Fig. 4). The x-axes in the BSPs are in units of substitution

	Lineage		
	North 2	São Paulo south	São Paulo north
Tajima's *D*	0.728	–1.0781	–1.423
P value	0.825	0.138	**0.051**
Fu's *Fs*	–0.331	–10.38	–23.07
P value	0.265	**0.014**	**< 0.0001**
Goodness-of-fit test			
SSD	—	0.004	0.0035
P value	—	**0.74**	**0.15**

Table 4 Estimates of Tajima's *D* (Tajima 1989), and Fu's *F* (Fu 1997) neutrality tests for population expansion in *Thoropa miliaris* and *T. taophora* population groups. In cases where expansion was evident based on either of those statistics, we applied a goodness-of-fit test based on sum of square deviations (SSD; Rogers & Harpending 1992; Schneider & Excoffier 1999). Nonsignificant values for SSD ($P > 0.05$) and significant negative *D* and *F* values are bolded

Table 5 Divergence time estimates for major nodes (A–C) and coalescence times for differentiation among haplotypes within mitochondrial clades (D–H) for the *Thoropa miliaris* complex. Mean time estimate values and 95% confidence intervals were inferred using three coalescent models and two data sets using BEAST (see text); estimates are reported in millions of years. Nodes A–H correspond to those in Figure 2

	Without islands			With islands		
Node/clade	Bayesian skyline	Exponential	Expansion	Bayesian Skyline	Exponential	Expansion
A	9.5 (7.8–11.4)	9.3 (7.6–11.1)	9.0 (7.3–10.7)	11.5 (9.6–12.4)	12.0 (9.8–13.2)	11.1 (9.2–12.3)
B	8.9 (7.1–10.9)	8.7 (6.9–10.7)	8.4 (6.5–10.3)	8.7 (6.7–10.9)	8.4 (6.3–10.6)	8.1 (5.6–11.2)
C	3.3 (2.4–4.2)	3.2 (2.4–4.0)	3.1 (2.3–3.9)	3.4 (2.6–4.4)	3.3 (2.4–4.2)	3.3 (2.1–4.4)
D – North 1	4.5 (3.3–5.7)	4.4 (3.2–5.6)	4.1 (3.0–5.4)	4.5 (3.3–5.8)	4.3 (3.0–5.5)	4.0 (2.6–5.4)
E – North 2	4.7 (3.4–5.9)	4.5 (3.3–5.8)	4.3 (2.9–5.5)	4.5 (3.3–5.8)	4.3 (3.1–5.5)	3.9 (2.4–5.3)
F – São Paulo south	0.5 (0.3–0.6)	0.5 (0.3–0.7)	0.5 (0.4–0.7)	1.1 (0.7–1.4)	1.0 (0.8–1.4)	1.1 (0.7–1.4)
G – São Paulo north	0.2 (0.1–0.3)	0.2 (0.15–0.3)	0.3 (0.2–0.4)	0.2 (0.2–0.3)	0.3 (0.2–0.4)	0.3 (0.2–0.4)
H – Juréia	0.2 (0.07–0.3)	0.2 (0.06–0.3)	0.2 (0.07–0.3)	0.2 (0.07–0.3)	0.2 (0.07–0.3)	0.2 (0.07–0.3)

per site and thus can be transformed to years before present by dividing by the mutation rate. We used the value 0.957% per lineage per million years, the substitution rate for the ND2 loci used in the timing analyses. According to BSP, after a prolonged period of constant population size, populations in clade North 2 appear to have experienced a slight decrease in size from about 145 000–450 000 BP followed by a demographic expansion beginning approximately 150 000–200 000 BP. We observed a similar pattern for the São Paulo south clade with a constant population size through time and subsequent demographic expansion beginning at 150 000 BP. Finally, populations from clade São Paulo north appear to have experienced an expansion phase throughout their entire history, beginning approximately 160 000 BP. All three lineages revealed a rapid expansion and constant population growth during the most recent time interval.

Discussion

Our analyses revealed significant diversity among lineages of *Thoropa miliaris* and *T. taophora* in northern and southern regions of the Atlantic Coastal Forest, as well as evidence that populations in the two regions have had very different evolutionary histories. Patterns of haplotype distribution in the two northern clades (in the states of Rio de Janeiro and Espírito Santo) indicate a complex history with potentially multiple northern refugia and subsequent population admixture. Our data suggest two possible scenarios, although our sampling in the north is not sufficient to differentiate between those two alternatives. First, if divergences of clades North 1 and North 2 occurred sequentially, as our topology indicates (Fig. 2), this could reflect a north-to-south colonization event early in the history of this species. Alternatively, if the two northern clades diverged simultaneously (as indicated by the broadly overlapping range estimates for TMRCA; Table 5), this might indicate isolation and divergence in independent northern refugia (one in Espírito Santo and one further south in Rio de Janeiro), followed by subsequent admixture between those two clades. In either case, the deeply divergent lineages present in northern Atlantic Forest suggest that combined, the region may have harboured one or more refugia, thus retaining genetic diversity and yielding the basal lineage divergences within this species. The exact nature and location of those refugia will differ by species (Carnaval *et al.* 2009), but the higher degree of genetic diversity among northern populations matches the prediction of population structure due to long-term persistence of population in stable refugia.

Our phylogenetic tree identified significant regional structure and deep divergences among five geographically structured clades. The greatest genetic structure and oldest divergences were found among northern populations (clades North 1 and North 2); these clades also show the highest genetic diversity (7–8% sequence divergence, and highest haplotype and nucleotide diversity). The deep divergences and structure of northern clades contrast markedly with the relatively low divergences of southernmost populations (São Paulo clades). This pattern is corroborated by the analysis of our single nuclear marker, despite lower overall genetic variability at that gene. This contrasting genetic structure in these two regions supports the model for historical habitat stability at higher latitudes of the Atlantic Forest biome (Carnaval & Moritz 2008; Carnaval *et al*. 2009).

The patterns of differentiation reflected in our topology are also evident in our distance-based analyses of population structure. A large proportion (70%) of the genetic variability in the *T. miliaris* complex can be explained by variance among regional groups of populations (Table 3). We attribute this primarily to deep divergences observed among distinct populations in the north, as well as between island and mainland populations in the São Paulo clades, many of which were identified as independent groups in our SAMOVA analysis. The high genetic variability among populations is also evident in the many significant pairwise F_{ST} values, suggesting low gene flow even among coastal populations. Population structure may result from the topographic complexity along the coast and the patchy distribution of appropriate habitat for this species (Feio 2002).

Combined, our data revealed that northern and southern Atlantic Coastal Forest carry the genetic signal of very different historical demographic processes. In the two northern groups, we found high nucleotide diversity (π) and high haplotypic diversity (h) indicating long evolutionary history in large stable populations (Grant & Bowen 1998). In contrast, the two southern São Paulo clades and Juréia show low nucleotide diversity and a high degree of haplotypic diversity, a genetic signature of expansion after a period of low effective population size (Grant & Bowen 1998). Our mismatch analyses corroborate this overall pattern of higher habitat stability in northern Atlantic Coastal Forest, with subsequent expansion into southern regions. Clade North 2, which includes haplotypes of northernmost populations, is the only clade for which we could statistically reject population expansion. The mismatch distribution for Clade North 2 is not unimodal (Fig. 4), however this distribution is based on relatively limited sampling compared to other clades, and thus should be interpreted with caution. In contrast, the signal of population expansion is evident in the well-sampled São Paulo clades north and south, using all measures of demographic change. Likewise, the Bayesian Skyline Plots reveal differences in the extent of historical demographic changes across the same three clades. The North 2 and São Paulo south clades (Fig. 4) show relative population size stability for approximately 3.5 million years and 500 000 years respectively, followed by precipitous increases in population size beginning 150 000–200 000 years ago. Clade North 2 from Espírito Santo shows a relatively moderate fivefold increase in population size over this time. In contrast, São Paulo south shows a 10-fold increase over the same time period and the São Paulo north shows a gradual increase in effective population size over its short history of 160 000 years. Dating of historical events from sequence data are based on a number of assumptions. As with all dating estimates, our results depend on the accuracy of the mutation rate we could obtain for our marker, therefore, these estimates should be interpreted with caution. Nonetheless, the population dynamics across regions of Atlantic Coastal Forest clearly have occurred in different time frames over the history of this species.

Based on (i) the inferred relative demographic stability during the history of clade North 2, (ii) the deep divergences among haplotypes in clades North 1 and 2, and (iii) the shallow population structure and evidence for recent population expansion in the southernmost Sao Paulo clades, we infer that ancestral populations belonging to the northern clades became isolated in one or more northern habitat refugia, and that one of these more northerly populations was the source for subsequent southward colonization into the state of São Paulo. However, our estimated divergence times, both of cladogenesis among lineages and population divergences within clades, revealed older lineage divergences than predicted by by recent paleomodeling approaches (Carnaval & Moritz 2008; Carnaval *et al*. 2009). While the paleomodels predict the persistence of stable forest refuges in northern Atlantic Forest during a Pleistocene dry phase 21 000 BP, our earliest estimated cladogenic event occurred in the Miocene approximately 4–10 million years ago for North 1 and North 2 lineages (Nodes D and E). The timing of population divergences within São Paulo clades are more recent, but still date to 300 000 to one million years ago (Table 5). Finally, the Bayesian Skyline Plots show that rapid increases in population size for the southernmost clades began 150 000–200 000 years ago. Thus, the habitat stability model (Carnaval & Moritz 2008) remains valid as a proxy for historical periods that might have had similar climates, but it is clear that the actual divergences among and within clades predate the most recent habitat changes in the Pleistocene.

Despite their relatively recent colonization from northern regions, populations of *T. taophora* in southern Atlantic Coastal Forest show some geographical genetic structure. Southern populations of *T. taophora* belong to three reciprocally monophyletic clades, São Paulo south (1.0–2.3

million years ago), São Paulo north (200 000–600 000 BP), and Juréia (200 000–300 000 BP). Our more extensive sampling among southern populations allows us to investigate potential barriers to gene flow at a finer scale in this region. Our topology revealed two clades composed of São Paulo haplotypes with a phylogeographical break between the localites BR101 km 6 (W) and BR101 wall 2 (Q). We identified higher genetic structure (as judged by branch lengths and posterior probabilities) among populations in the clade São Paulo south, which includes primarily southern São Paulo localities. We also found an earlier age of diversification for populations within this clade (1.0–2.3 million years ago), suggesting that the north to south expansion hypothesis yielding successively younger divergences does not apply to populations within the southern Atlantic Coastal Forest. The São Paulo coastline is topographically complex and has had a highly erratic history due to tectonic activity and sea-level changes associated with glacial cycles (Suguio & Martin 1978). These historic complexities in the landscape have likely played important roles in the distribution of habitat availability and even possibly resulted in southern refugial populations that later recolonized more northern São Paulo coastline as habitat expanded during glacial recessions in the Pleistocene. This hypothesis is corroborated by the BSP estimates of demographic expansions that indicate populations in clade São Paulo north have a short history, and expanded in size only very recently.

In addition to climatic cycles that affected the distribution of forest habitats, dramatic historical landscape changes also occurred due to repeated oceanic incursions associated with changes in sea level (Suguio & Martin 1978). These sea level transgressions and regressions resulted in the repeated isolation of the highest elevation points along the coast (Suguio & Martin 1978; Suguio *et al*. 2005). The eastern coastline of Brazil is not uniform and in São Paulo, latitudinal differences in geomorphology of the coastline resulted in different isolation histories throughout the state (Suguio & Martin 1978). We sampled *Thoropa* from populations on continental islands along the São Paulo coast that were last connected to the mainland during marine regressions in the Holocene (Souza *et al*. 2005). Haplotypes from the four island populations in the less diverged São Paulo north clade (Ilha Prumirim, Ilha das Couves Norte, Ilha Redonda, Ilha de Porcos Pequena) do not form monophyletic groups. In contrast, haplotypes from three out of four islands off the southern São Paulo coast form well-supported monophyletic groups in our topology (Ilha de São Sebastião, Ilha dos Gatos, Ilha das Couves Sul). In each case, the sister taxon of an island clade is a nearby, if not the closest, mainland population. This regional disparity in genetic structure of island populations highlights the non-uniform effects of sea level changes along this topographically complex São Paulo coastline. Local vicariant events caused by rising sea levels, caused different degrees of insularity. In some taxa, the isolation has been sufficient to result in speciation of insular species (Marques *et al*. 2002; Brasileiro *et al*. 2007a, b, c). Fine-scale analyses using microsatellites to test for differentiation among island and coastal populations of *Thoropa taophora* throughout São Paulo state are currently underway in our laboratory (MC Duryea, CA Brasileiro, KR Zamudio, unpublished data).

Our results underscore the long-term effects of historical isolation for genetic population variability, even in the absence of current isolating mechanisms. Both mitochondrial and nuclear analyses revealed significant genetic differentiation of samples from Juréia relative to all other São Paulo populations. This site is composed of a high-elevation massif that was historically an island, separated from the coast under conditions of higher sea levels in the Pleistocene and Holocene (Suguio 2004; Pombal & Gordo 2004). The current coastal lowlands and mid-elevation regions are appropriate habitat for *Thoropa*. The samples we collected there form a strongly supported clade sister to all other São Paulo populations. This pattern may be in part due to isolation by distance and a sampling gap between Juréia and other São Paulo samples; however, this region is a known location of high endemicity and diversification due to its isolated history. Therefore, Juréia may have been one possible southern refuge for populations of *T. taophora* during times of higher sea level. Populations have remained isolated in this region, despite the current connection to the mainland. The deep divergence of these haplotypes corroborate that this refugium continues to be, effectively, an island, perhaps due to the lack of suitable habitat in the lowland valleys that currently surround the previously insular massif.

The genetic structure we uncovered within the *T. miliaris* complex supports the recent taxonomic decision to recognize southern and northern populations as distinct species (*T. miliaris* and *T. taophora*; Feio *et al*. 2006). However, our phylogenetic analysis shows that *T. miliaris* (clades North 1 and North 2) is a paraphyletic taxon. Although taxonomic recommendations are not the main goal of this study, we suggest that extreme levels of divergence among northern populations of *T. miliaris* reflect potential species-level differences. Indeed, some evidence of phenotypic differentiation exists among geographical regions within *T. miliaris* and *T. taophora*, suggesting a need for further taxonomic reconsideration of diversification within the two species.

Our study is one of the first to evaluate the distribution of genetic diversity among amphibian populations in southern regions of the Atlantic Coastal Forest. Phylogeographic studies of other vertebrate taxa show mixed support for the prediction of higher diversity in northern Atlantic Forest but all show unique regional differences in genetic structure (Costa 2003; Leite 2003; Pellegrino *et al*.

2005; Grazziotin *et al*. 2006; Cabanne *et al*. 2007). These inconsistencies are in agreement with other findings that suggest diversification patterns are not uniform across Atlantic Coastal Forest taxa (Costa 2003; Lara *et al*. 2005). A lack of phylogeographical congruence could be caused by differences in levels of gene flow, response of species to the same environmental or geographical feature, or differences in effective population sizes (Zink *et al*. 2001). Comparative phylogeography across a broad range of taxa is thus necessary to uncover large-scale patterns underlying diversity in such a complex region (Rull 2008).

Our data reveal patterns of geographical variation in genetic structure indicating that historical distribution of habitat, topographic complexity, and historical fragmentation have played important roles in divergences within the *T. miliaris* species complex, even in southern Atlantic Coastal Forest regions that have been colonized more recently. Regional differences in the degree of genetic structuring are concordant with historical predictions of habitat distribution (Carnaval & Moritz 2008). However, our data also underscore how rapidly habitat distribution can alter genetic connectivity among populations in this landscape. Despite its shorter history, the southern region already shows divergences associated with discontinuities in the coastal landscape, and periods of population isolation due to climate and sea level changes. We propose that it is this dynamic nature of recent regional differences in geologic activity combined with continued historical changes in habitat distribution due to climatic effects that has contributed to diversification of Atlantic Coastal Forest biota.

The Atlantic Coastal Forest has endured crisis-level habitat loss over the past seven decades, threatening biodiversity and species endemic to this biome (Morellato & Haddad 2000; Myers *et al*. 2000). Studies of genetic diversity among regions in this fragmented landscape are crucial for conservation planning and prioritization. Genetic analyses reveal regions where independent lineages, each with its own evolutionary potential, should be maintained. Our data corroborate that habitat protection in northern Atlantic Forest should be of high priority because of the presumed refugia and historically high rates of diversification in this region. Despite its importance, deforestation rates and anthropogenic influence in the north are significantly higher than in other parts of Atlantic Coastal Forest (Fundação SOS Mata Atlântica 1992). However, our data also highlight more recent evolutionary processes leading to diversification in southern Atlantic Forest suggesting this region also plays an important role in generating and preserving biodiversity. Further studies of taxa endemic to the Atlantic Coastal Forest will provide windows into the generality of historical processes that led to geographically localized hotspots in biodiversity.

Acknowledgements

Samples were collected under permits #119 (2005–2006) and #11457–1 (2007) issued by the Instituto Brasileiro do Meio Ambiente e dos Recursos Naturais Renováveis (IBAMA) and exported under export licenses #0116729 BR and #0121653 BR issued by the Ministério do Meio Ambiente/IBAMA. We thank the Instituto de Biociências at the Universidade de São Paulo; Museu de História Natural at the Universidade Estadual de Campinas, Instituto Florestal de São Paulo, and Reserva Santa Lúcia for logistical support. We thank E. Lucas, F. Centeno, F. R. de Campos, H. M. Oyamaguchi, J. L. Gasparini, L. Francini, M. T. Thomé, N. L. Hulle, M. Segalla, M. R. C. Martins, R. J. Sawaya, S. Buzatto for help with sample collections, J. Pombal Jr. and M.T. Rodrigues for donation of tissues, and C. G. Becker for preparing Fig. 1. A. DeWoody, E. Fischer, J. Fitzpatrick, I. Lovette and members of the Zamudio laboratory provided valuable feedback on analyses and previous versions of this manuscript. Molecular data were collected in the Evolutionary Genetics Core Facility at Cornell University and MrBayes runs were performed at Cornell's Computational Biology Service Unit, a facility partially funded by Microsoft Corporation. Funding for this project was provided by grants and fellowships from the Cornell Hughes Scholar Program 2007, Dextra Undergraduate Research Endowment, CALS Honors Research Fund (to S.F.), Fundação de Amparo à Pesquisa do Estado de São Paulo (FAPESP), Conselho Nacional do Desenvolvimento Científico e Tecnológico, Fundação Boticário para Proteção da Natureza, Coordenação de Aperfeiçoamento de Pessoal de Nível Superior (to C.F.B.H. and C.A.B.), and the National Science Foundation Biotic Survey and Inventory Program (to K.Z.).

References

Abe AS, Bicudo J (1991) Adaptations to salinity and osmoregulation in the frog *Thoropa miliaris* (Amphibia, Leptodactylidae). *Zoologischer Anzeiger*, **227**, 313–318.

Behling H, Negrelle RRB (2001) Tropical rain forest and climate dynamics of the Atlantic lowland, Southern Brazil, during the late Quaternary. *Quaternary Research*, **56**, 383–389.

Bokermann WCA (1965) Notas sobre as espécies de *Thoropa* Fitzinger (Amphibia, Leptodactylidae). *Anais da Academia Brasileira de Ciências*, **37**, 525–537.

Brasileiro CA, Haddad CFB, Sawaya RJ, Sazima I (2007a) A new and threatened island-dwelling species of *Cycloramphus* (Anura: Cycloramphidae) from southeastern Brazil. *Herpetologica*, **63**, 501–510.

Brasileiro CA, Oyamaguchi HM, Haddad CFB (2007b) A new island species of *Scinax* (Anura; Hylidae) from southeastern Brazil. *Journal of Herpetology*, **41**, 271–275.

Brasileiro CA, Sawaya RJ, Martins M, Haddad CFB (2007c) A new and threatened species of *Scinax* (Anura: Hylidae) from Queimada Grande Island, southeastern Brazil. *Zootaxa*, **1391**, 47–55.

Brown KS Jr, Brown GG (1992) Habitat alteration and species loss in Brazilian forests. In: *Tropical Deforestation and Species Extinction* (ed. Whitmore TC, Sayer JA), pp. 120–142. Chapman & Hall, London.

Brown WM, Prager EM, Wang A, Wilson AC (1982) Mitochondrial DNA sequences of primates: tempo and mode of evolution. *Journal of Molecular Evolution*, **18**, 225–239.

Cabanne GS, Santos FR, Miyaki CY (2007) Phylogeography of *Xiphorhynchus fuscus* (Passeriformes, Dendrocolaptidae): vicariance and recent demographic expansion in southern Atlantic Forest. *Biological Journal of the Linnean Society*, **91**, 73–84.

Carey C, Alexander MA (2003) Climate change and amphibian declines: is there a link? *Diversity and Distributions*, **9**, 111–121.

Carnaval AC (2002) Phylogeography of four frog species in forest fragments of northeastern Brazil – a preliminary study. *Integrative and Comparative Biology*, **42**, 913–921.

Carnaval AC, Bates JM (2007) Amphibian DNA shows marked genetic structure and tracks Pleistocene climate change in northeastern Brazil. *Evolution*, **61**, 2942–2957.

Carnaval AC, Moritz CM (2008) Historical climate modeling predicts patterns of current biodiversity in the Brazilian Atlantic Forest. *Journal of Biogeography*, **35**, 1187–1201.

Carnaval AC, Hickerson MJ, Haddad CFB, Rodrigues MT, Moritz CM (2009) Stability predicts genetic diversity in the Brazilian Atlantic Forest hotspot. *Science*, **323**, 785–789.

Caruso F, Suguio K, Nakamura T (2000) The Quaternary geological history of the Santa Catarina southeastern region (Brazil). *Anais da Academia Brasileira de Ciências*, **72**, 257–270.

Clement M, Posada D, Crandall K (2000) TCS: a computer program to estimate gene genealogies. *Molecular Ecology*, **9**, 1657–1660.

Costa LP (2003) The historical bridge between the Amazon and the Atlantic Forest of Brazil: a study of molecular phylogeography with small mammals. *Journal of Biogeography*, **30**, 71–86.

Costa LP, Leite YLR, da Fonseca GAB, da Fonseca MT (2000) Biogeography of South American forest mammals: endemism and diversity in the Atlantic Forest. *Biotropica*, **32**, 872–881.

Crawford AJ (2003) Huge populations and old species of Costa Rican and Panamanian dirt frogs inferred from mitochondrial and nuclear gene sequences. *Molecular Ecology*, **12**, 2525–2540.

Drummond AJ, Rambaut A (2007) BEAST: Bayesian evolutionary analysis by sampling trees. *BMC Evolutionary Biology*, **7**, 214.

Drummond AJ, Nicholls GK, Rodrigo AG, Solomon W (2002) Estimating mutation parameters, population history and genealogy simultaneously from temporally spaced sequence data. *Genetics*, **161**, 1307–1320.

Drummond AJ, Rambaut A, Shapiro B, Pybus OG (2005) Bayesian coalescent inference of past population dynamics from molecular sequences. *Molecular Biology* and *Evolution*, **22**, 1185–1192.

Dupanloup I, Schneider S, Excoffier L (2002) A simulated annealing approach to define the genetic structure of populations. *Molecular Ecology*, **11**, 2571–2581.

Excoffier L, Smouse P, Quattro J (1992) Analysis of molecular variance inferred from metric distances among DNA haplotypes: application to human mitochondrial DNA restriction data. *Genetics*, **131**, 479–491.

Feio RN (2002) *Revisão taxonômica O, gênero Thoropa Cope, 1865 (Amphibia, Anura, Leptodactylidae)*. PhD Thesis. Museu Nacional, Rio de Janeiro, Brazil.

Feio RN, Napoli MF, Caramaschi U (2006) Taxonomic consideration of *Thoropa miliaris* (Spix, 1824) with revalidation and redescription of *Thoropa taophora* (Miranda-Ribeiro, 1923) (Amphibia, Anura, Leptodactylidae). *Arquivos do Museu Nacional, Rio de Janeiro*, **64**, 41–60.

Frost DR, Grant T, Faivovich J *et al*. (2006) The amphibian tree of life. *Bulletin of the American Museum of Natural History*, **297**, 1–370.

Fu XY (1997) Statistical tests of neutrality of mutations against population growth, hitchhiking, and background selection. *Genetics*, **147**, 915–925.

Fundação SOS Mata Atlântica (1992) *Dossier Atlantic Rainforest (Mata Atlântica) 1992*. Fundação SOS Mata Atlantica, São Paulo, Brazil.

Gatesy J, DeSalle R, Wheller W (1993) Alignment-ambiguous nucleotide sites and the exclusion of systematic data. *Molecular Phylogenetics* and *Evolution*, **2**, 152–157.

Giaretta AA, Facure KG (2004) Reproductive ecology and behavior of *Thoropa miliaris* (Spix, 1824) (Anura, Leptodactylidae, Telmatobiinae). *Biota Neotropica*, **4**, 1–10.

Glor RE, Vitt LJ, Larson A (2001) A molecular phylogenetic analysis of diversification in Amazonian *Anolis* lizards. *Molecular Ecology*, **10**, 2661–2668.

Goebel AM, Donnelly JM, Atz ME (1999) PCR primers and amplification methods for 12S ribosomal DNA, the control region, cytochrome oxidase I, and cytochrome b in bufonids and other frogs, and an overview of PCR primers which have amplified DNA in amphibians successfully. *Molecular Phylogenetics* and *Evolution*, **11**, 163–199.

Grant WS, Bowen BW (1998) Shallow population histories in deep evolutionary lineages of marine fishes: insights from Sardines and Anchovies and lessons for conservation. *The Journal of Heredity*, **85**, 415–426.

Grazziotin FG, Monzel M, Echeverrigaray S, Bonatto SL (2006) Phylogeography of the *Bothrops jararaca* complex (Serpentes: Viperidae): past fragmentation and island colonization in the Brazilian Atlantic Forest. *Molecular Ecology*, **15**, 3969–3982.

Haddad CFB, Prado CPA (2005) Reproductive modes in frogs and their unexpected diversity in the Atlantic Forest of Brazil. *Bioscience*, **55**, 724–724.

Haffer J (1969) Speciation in Amazonian Forest Birds. *Science*, **165**, 131.

Haffer J, Prance GT (2001) Climatic forcing of evolution in Amazonia during the Cenozoic: on the refuge theory of biotic differentiation. *Amazoniana-Limnologia Et Oecologia Regionalis Systemae Fluminis Amazonas*, **16**, 579–605.

Hasegawa M, Kishino H, Yano TA (1985) Dating of the human-ape splitting by a molecular clock of mitochondrial DNA. *Journal of Molecular Evolution*, **22**, 160–174.

Huelsenbeck JP, Ronquist F (2001) MrBayes: Bayesian inference of phylogenetic trees. *Bioinformatics*, **17**, 754–755.

Lara MC, Patton JL (2000) Evolutionary diversification of spiny rats (genus *Trinomys*, Rodentia: Echimyidae) in the Atlantic Forest of Brazil. *Zoological Journal of the Linnean Society*, **130**, 661–686.

Lara MC, Geise L, Schneider CJ (2005) Diversification of small mammals in the Atlantic forest of Brazil: testing the alternatives. In: *Mammalian Diversification: from Chromosomes to Phylogeography (a Celebration of the Career of James A. Patton* (eds Lacey EA, Myers P), pp. 311–331. University of California Publications in Zoology, University of California, Berkeley, California.

Ledru MP, Salgado-Labouriau ML, Lorscheitter ML (1998) Vegetation dynamics in southern and central Brazil during the last 10 000 yr. *B.P. Review of Palaeobotany and Palynology*, **99**, 131–142.

Leite YLR (2003) Evolution and systematics of the Atlantic tree rats, genus *Phyllomys* (Rodentia, Echimyidae), with description of two new species. *University of California Publications in Zoology*, **132**, 1–118.

Macey JR, Larson A, Ananjeva NB, Fang ZL, Papenfuss TJ (1997) Two novel gene orders and the role of light-strand replication in rearrangement of the vertebrate mitochondrial genome. *Molecular Biology* and *Evolution*, **14**, 91–104.

Marques OAV, Duleba W (2004) *Estação Ecológica Juréia-Itatins: Ambiente Físco, Flora e Fauna*. Holos, Ribeirão Preto, São Paulo, Brazil.

Marques OAV, Martins M, Sazima I (2002) A new insular species of pitviper from Brazil, with comments on evolutionary biology and conservation of the *Bothrops jararaca* group (Serpentes, Viperidae). *Herpetologica*, **58**, 303–312.

Martins LR, Coutinho PN (1981) The Brazilian continental margin. *Earth-Science Reviews*, **17**, 87–107.

Morellato LPC, Haddad CFB (2000) Introduction. *The Brazilian Atlantic Forest. Biotropica*, **32**, 786–792.

Moritz C, Patton JL, Schneider CJ, Smith TB (2000) Diversification of rainforest faunas: an integrated molecular approach. *Annual Review of Ecology* and *Systematics*, **31**, 533–563.

Myers N, Mittermeier RA, Mittermeier CG, da Fonseca GAB, Kent J (2000) Biodiversity hotspots for conservation priorities. *Nature*, **403**, 853–858.

Nei M (1987) *Molecular Evolutionary Genetics*. Columbia University Press, New York.

Pellegrino KCM, Rodrigues MI, Waite AN (2005) Phylogeography and species limits in the *Gymnodactylus darwinii* complex (Gekkonidae, Squamata): genetic structure coincides with river systems in the Brazilian Atlantic Forest. *Biological Journal of the Linnean Society*, **85**, 13–26.

Pinto-da-Rocha R, da Silva MB (2005) Faunistic similarity and historic biogeography of the harvestment of southern and southeastern Atlantic Rain Forest of Brazil. *The Journal of Arachnology*, **33**, 290–299.

Pizo MA, Oliveira PS (2000) The use of fruits and seeds by ants in the Atlantic forest of southeast Brazil. *Biotropica*, **32**, 851–861.

Pombal JP, Gordo M (2004) Anfíbios anuros da Juréia. In: *Estação Ecológica Juréia-Itatins, Ambiente Físico, Flora E Fauna* (eds Marques OAV, Duleba W), pp. 243–256. Holos Editora, Ribeirão Preto.

Posada D, Crandall KA (1998) ModelTest: testing the model of DNA substitution. *Bioinformatics*, **14**, 817–818.

Prychitko TM, Moore WS (1997) The utility of DNA sequences of an intron from the beta-fibrinogen gene in phylogenetic analysis of woodpeckers (Aves: Picidae). *Molecular Phylogenetics* and *Evolution*, **8**, 193–204.

Rambaut A, Drummond A (2004) *Tracer. MCMC Trace Analysis Tool, Version 1.3*. University of Oxford, Oxford, UK.

Ribas CC, Miyaki C (2004) Molecular systematics in *Aratinga* parakeets: species limits and historical biogeography in the 'solstitialis' group, and the systematic position of *Nadayus nenday*. *Molecular Phylogenetics* and *Evolution*, **30**, 663–675.

Rodriguez F, Oliver JL, Marin A, Medina JR (1990) The general stochastic model of nucleotide substitution. *Journal of Theoretical Biology*, **142**, 485–501.

Rogers A, Harpending H (1992) Population growth makes waves in the distribution of pairwise genetic differences. *Molecular Biology* and *Evolution*, **9**, 552–569.

Rull V (2008) Speciation timing and neotropical biodiversity: the Tertiary-Quaternary debate in the light of molecular phylogenetic evidence. *Molecular Ecology*, **17**, 2722–2729.

Sazima I (1971) The occurrence of marine invertebrates in the stomach contents of the frog *Thoropa miliaris*. *Ciência e Cultura*, **23**, 647–648.

Schneider S, Excoffier L (1999) Estimation of past demographic parameters from the distribution of pairwise differences when the mutation rates vary among sites: application to human mitochondrial DNA. *Genetics*, **152**, 1079–1089.

Schneider S, Roessli D, Excoffier L (2000) *Arlequin, A Software for Population Genetic Data Analysis*, Version 3.01. Genetics and Biometry Laboratory, University of Geneva, Switzerland.

da Silva JMC, de Sousa MC, Castelletti CHM (2004) Areas of endemism for passerine birds in the Atlantic forest, South America. *Global Ecology and Biogeography*, **13**, 85–92.

Simpson BB (1979) Quaternary biogeography of the high montane regions of South America. In: *The South American Herpetofauna: its Origin, Evolution, and Dispersal* (ed. Duellman WE), pp. 157–188. Monograph of the Museum of Natural History, University of Kansas, Lawrence, Kansas.

Siqueira CC, Van Sluys M, Ariani CV, Rocha CFD (2006) Feeding ecology of *Thoropa miliaris* (Anura, Cycloramphidae) in four areas of Atlantic Rain Forest, southeastern Brazil. *Journal of Herpetology*, **40**, 520–525.

Souza CR, Suguio K, Oliveira AM, Oliveira PE (2005) *Quaternário do Brasil*. Holos, Ribeirão Preto, São Paulo, Brazil.

Stephens M, Donnelly P (2003) A comparison of Bayesian methods for haplotype reconstruction from population genotype data. *American Journal of Human Genetics*, **73**, 1162–1169.

Stephens M, Smith NJ, Donnelly P (2001) Comparisons of two methods for haplotype reconstruction and haplotype frequency estimation from population data. *American Journal of Human Genetics*, **69**, 912–914.

Suguio K (2004) O papel das variações do nível relativo do mar durante o Quaternário Tardio na origem da baixada litorânea da Juréia, SP. In: *Estação Ecológica Juréia-Itatins: Ambiente Físco, Flora E Fauna* (ed. Marques OAV, Duleba W). Holos, Ribeirão Preto, São Paulo, Brazil.

Suguio K, Martin L (1978) Quaternary marine formations of the states of São Paulo and southern Rio de Janeiro. In: *International Symposium on Coastal Evolution in the Quaternary*, p. 55. University of São Paulo, São Paulo, Brazil.

Suguio K, Angulo RJ, Corrêa ICS, Tomazelli LJ, Willwock JA, Vital H (2005) Paleoníveis do mar e paleolíneas de costa. In: *Quaternário Do Brasil* (eds Souza CR, Suguio K, Oliveira AM, Oliveira PE). Holos, Ribeirão Preto, São Paulo, Brazil.

Swofford DL (2002) *PAUP* Phylogenetic Analysis Using Parsimony (* and Other Methods)*. Sinauer & Associates, Sunderland, Massachusetts.

Tajima F (1983) Evolutionary relationship of DNA sequences in finite populations. *Genetics*, **105**, 437–460.

Tajima F (1989) Statistical method for testing the neutral mutational hypothesis by DNA polymorphism. *Genetics*, **123**, 585–595.

Tamura K (1992) Estimation of the number of nucleotide substitutious when there are strong transition–transversion and G + content biases. *Molecular Biology and Evolution*, **9**, 678–687.

Templeton A, Crandall K, Sing C (1992) A cladistic analysis of phenotypic associations with haplotypes inferred from restriction endonuclease mapping and DNA sequence data. *Genetics*, **132**, 597–601.

Thompson JD, Higgins DG, Gibson TJ (1994) ClustalW: improving the sensitivity of progressive multiple sequence alignment through sequence weighting, position-specific gap penalties and weight matrix choice. *Nucleic Acids Research*, **22**, 4673–4680.

Vanzolini PE, Williams EE (1981) The vanishing refuge: a mechanism for ecogeographic speciation. *Papeis Avulsos de Zoologia*, **34**, 251–255.

Vences M, Kosuch J, Lotters S *et al*. (2000) Phylogeny and classification of poison frogs (Amphibia: Dendrobatidae), based on mitochondrial 16S and 12S ribosomal RNA gene sequences. *Molecular Phylogenetics* and *Evolution*, **15**, 34–40.

Wüster W, Ferguson JE, Quijada-Mascareñas JA *et al*. (2005) Tracing an invasion: landbridges, refugia, and the phylogeography of the neotropical rattlesnake (Serpentes: Viperidae: *Crotalus durissus*). *Molecular Ecology*, **14**, 1095–1108.

Zink RM, Kessen AE, Line TV, Blackwell-Rago RC (2001) Comparative phylogeography of some aridland bird species. *Condor*, **103**, 1–10.

Zink PM, Klicka J, Barber BR (2004) The tempo of avian diversification during the Quaternary. *Philosophical Transactions of the Royal Society London B*, **359**, 215–220.

Sarah Fitzpatrick is currently a PhD student at Colorado State University interested in evolutionary ecology, and mechanisms underlying phenotypic and genetic diversity in amphibians and fishes. This research was conducted in partial fulfillment of her Undergraduate Honor's Thesis at Cornell University. The research of Cinthia Brasileiro and Célio Haddad focuses on diversification and conservation of Brazilian amphibians, with emphasis on frogs endemic to Atlantic Coastal Forest. The Zamudio Laboratory studies patterns and mechanisms of population divergence, historical phylogeography, and conservation of New World reptiles and amphibians.

Supporting information

Additional supporting information may be found in the online version of this article:

Table S1 Pairwise population F_{ST} values among populations of *Thoropa miliaris* species complex

Please note: Wiley-Blackwell are not responsible for the content or functionality of any supporting materials supplied by the authors. Any queries (other than missing material) should be directed to the corresponding author for the article.

Appendix

Sampling localities and coordinates, sample size (*N*) and mtDNA haplotype ID for sampled populations of *Thoropa miliaris* and *Thoropa taophora*. Superscript numbers indicate the frequency of individuals corresponding to the given haplotype. Voucher specimens for nuclear and mitochondrial sequences have been deposited at the Coleção de Anfíbios, Universidade Estadual Paulista — UNESP, Rio Claro, Brazil (CFBH), Museu Nacional Rio de Janeiro (MNRJ), or private tissue collections (AF; MTR). Nuclear and mitochondrial sequences have been deposited in GenBank (accession nos GQ174521–GQ175057)

Site	Taxon	Locality	State	Coordinates	*N*	Mitochondrial DNA haplotype ID	Mitochondrial voucher no.	Nuclear voucher no.
A	*Thoropa miliaris*	Vale da Revolta	RJ	21°46′10″S 42°32′47″S	1	A1[1]	MNRJ 44566	—
B	*Thoropa miliaris*	Petrópolis	RJ	22°32′14.46″S 43°14′1.82″W	6	B2[1], B3[1], B4[1]	CFBH10125, tadpoles (2)	CFBH10125, tadpoles (4)
C	*Thoropa miliaris*	Domingos Martins	ES	20°26′07.2″S 41°01′17.4″W	6	C5[1], C6[1], C7[1], C8[1], C9[1], C10[1]	tadpoles (2), CFBH11329, CFBH18430-18432	CFBH18432
D	*Thoropa miliaris*	Reserva Santa Lúcia, Santa Tereza	ES	19°57′32.9″S 40°32′24.3″W	8	D11[1], D12[1], D13[1], D14[1], D15[1], D16[1], D17[1], D18[1]	CFBH14972, CFBH14975-14977, CFBH18011, CFBH18014, CFBH18448-18449	—
E	*Thoropa miliaris*	Canto da Praia, Vitória	ES	20°18′12.9″S 40°17′42.7″W	4	E19[1], E20[1], E21[1], E22[1]	CFBH18437, CFBH18439, CFBH18442, CFBH18446	CFBH18437, CFBH18442, CFBH18446
F	*Thoropa taophora*	Rio Verde, Estação Ecológica Juréia-Itatins	SP	24°33′00″S 47°13′16″W	7	F26[1], F27[1], F28[1], F29[1], F30[1]	CFBH10911, CFBH10914, CFBH10916, CFBH13796, CFBH13798	CFBH10911, CFBH10914, CFBH10916-10917, CFBH13796-13798
G	*Thoropa taophora*	Ilha de São Sebastião/ Parque Estadual da Ilhabela	SP	23°49′52″S 45°21′10″W	3	G31[1], G32[1], G33[1]	CFBH15323-15325	CFBH15322, CFBH15324-15325
H	*Thoropa taophora*	Santos	SP	23°50′50″S 46°21′56″W	1	H34[1]	MTR 9371	MTR 9371
I	*Thoropa taophora*	Barra do Una	SP	23° 44′27″S 45°45′01″W	7	I35[1], I36[3], I37[1], I38[1]	CFBH10920, CFBH10929, CFBH10931, CFBH10933, CFBH10952, CFBH12108	CFBH10920, CFBH10926, CFBH10927-10928, CFBH10931, CFBH10933, CFBH10952
J	*Thoropa taophora*	Ilha de Toque Toque	SP	23°50′04″S 45°31′19″W	5	J39[3], J40[2]	CFBH15707-15708, CFBH15585, CFBH15589-5590	CFBH15707-15708, CFBH15585, CFBH15589-15590
K	*Thoropa taophora*	Ilha dos Gatos	SP	23°48′16″S 45°40′05″W	5	K41[1], K42[1], K43[1], K44[1], K45[1]	CFBH15685, CFBH15687, CFBH15694, CFBH15696, CFBH20170	CFBH15694
L	*Thoropa taophora*	Ilha Tamanduá	SP	23°35′39″S 45°17′28″W	4	L46[3], L47[1]	CFBH12612, CFBH19715, CFBH20168-20169	CFBH12612, CFBH19722, CFBH20168
M	*Thoropa taophora*	BR101 Rodovia Rio-Santos, stream km 27, Núcleo Picinguaba, Parque Estadual da Serra do Mar	SP	23°21′45″S 44°57′11″W	4	M48[1], M49[1], M50[1], M76[1]	CFBH7941, CFBH7945-7947	CFBH7945-7946

Appendix *Continued*

Site	Taxon	Locality	State	Coordinates	*N*	Mitochondrial haplotype ID	Mitochondrial voucher no.	Nuclear voucher no.
N	*Thoropa taophora*	Praia da Sununga	SP	23°30′34.8″S 45°07′54.5″W	6	N51[1], N52[1], N53[1], N54[1], N55[1]	tadpoles (5)	tadpoles (5)
O	*Thoropa taophora*	Praia Domingas Dias	SP	23°29′47.0″S 45°08′46.0″W	5	O56[1], O57[3], O58[1]	tadpoles (5)	tadpoles (5)
P	*Thoropa taophora*	BR101 Rodovia Rio-Santos, wall km 16.9, Núcleo Picinguaba, Parque Estadual da Serra do Mar	SP	23°19′14″S 44°53′11″W	7	P59[1], P60[2], P61[2], P62[1]	tadpoles (6)	tadpoles (7)
Q	*Thoropa taophora*	BR101 Rodovia Rio-Santos, wall km 19.2, Núcleo Picinguaba, Parque Estadual da Serra do Mar	SP	23°21′34″S 44°56′42″W	6	Q63[1], Q64[1], Q65[1], Q66[3]	tadpoles (6)	tadpoles (6)
R	*Thoropa taophora*	Trilha Petrobrás, Núcleo Caraguatatuba, Parque Estadual da Serra do Mar	SP	23°41′3.30″S 45°39′7.17″W	1	R67[1]	CFBH12894	CFBH12894
S	*Thoropa taophora*	Ilha das Couves Sul	SP	23°48′07″S 45°43′32″W	6	S68[1], S69[4]	CFBH15701, CFBH15605-15607, CFBH15609	CFBH15701, CFBH15604-15607, CFBH15609,
T	*Thoropa taophora*	Itaguá, Ubatuba	SP	23°27′26.2″S 45°03′06.7″W	5	T70[3], T71[2]	tadpoles (5)	tadpoles (3)
U	*Thoropa taophora*	Trilha Mococa, Núcleo Caraguatatuba, Parque Estadual da Serra do Mar	SP	23°33′37″S 45°18′23″W	1	U72[1]	CFBH12142	CFBH12142
V	*Thoropa taophora*	Cachoeira Prumirim	SP	23°22′30″S 44°57′55″W	2	V73[1], V74[1]	CFBH7942-7943	CFBH7942-7943
W	*Thoropa taophora*	BR101 Rodovia Rio-Santos, stream km 34.5, Núcleo Picinguaba, Parque Estadual da Serra do Mar		23°23′21″S 44°59′29″W	1	W75[1]	CFBH7948	CFBH7948
X	*Thoropa taophora*	Ilha Prumirim	SP	23°23′05″S 44°56′49″W	9	X77[1], X78[3], X79[3]	CFBH10466, CFBH10469, CFBH12635, CFBH15661-15662, CFBH15658-15659,	CFBH10466, CFBH10468-10469, CFBH12635, CFBH15658-15662
Y	*Thoropa taophora*	Ilha das Couves Norte	SP	23°25′23″S 44°51′19″W	5	Y80[1],Y81[1], Y82[1], Y83[1], Y84[1]	CFBH12607, CFBH12616-12619	CFBH12607, CFBH12616-12619
Z	*Thoropa taophora*	Ilha Redonda	SP	23°21′07″S 44 54′16″W	9	Z85[1], Z86[1], Z87[1], Z88[1], Z89[1], Z90[1], Z91[1]	CFBH10472, CFBH10474, CFBH10476, CFBH10479, CFBH15602, CFBH15647, CFBH15654	CFBH10472, CFBH10474, CFBH10476, CFBH10479, CFBH15600, CFBH15602, CFBH15647, CFBH15654, CFBH15682,

Appendix *Continued*

Site	Taxon	Locality	State	Coordinates	*N*	Mitochondrial haplotype ID	Mitochondrial voucher no.	Nuclear voucher no.
aa	*Thoropa taophora*	BR101 Rodovia Rio-Santos, stream km 3, Núcleo Picinguaba, Parque Estadual da Serra do Mar	SP	23°21′36″S 44°46′59″W	5	aa92[1], aa93[1], aa94[2]	CFBH07980, tadpoles (3)	CFBH07980, tadpoles (4)
bb	*Thoropa taophora*	Praia Brava da Almada	SP	23°21′48″S 44°52′56″W	5	bb95[1], bb96[1], bb97[1], bb98[1]	tadpoles (4)	tadpoles (5)
cc	*Thoropa taophora*	BR101 Rodovia Rio-Santos, wall km 3, Núcleo Picinguaba, Parque Estadual da Serra do Mar	SP	23°21′37″S 44°46′37″W	5	cc99[2], cc100[1], cc101[1]	tadpoles (4)	tadpoles (5)
dd	*Thoropa taophora*	BR101 Rodovia Rio-Santos, stream km 3.5, Núcleo Picinguaba, Parque Estadual da Serra do Mar	SP	23°21′39.5″S, 44°47′12.1″W	1	dd102[1]	tadpole (1)	tadpole (1)
ee	*Thoropa taophora*	Vietnam trail, Núcleo Picinguaba, Parque Estadual da Serra do Mar	SP	23°21′12″S 44°50′45″W	6	ee103[2], ee104[1]	tadpoles (3)	tadpoles (3)
ff	*Thoropa taophora*	Headquarters, Núcleo Picinguaba, Parque Estadual da Serra do Mar	SP	23°21′52.0″S 44°49′30.3″W	1	ff105[1]	tadpole (1)	tadpole (1)
gg	*Thoropa taophora*	Ilha de Porcos Pequena	SP	23°22′35″S 44°54′07″W	7	gg106[5]	CFBH7644-7645, CFBH10940, CFBH10944, CFBH10949	CFBH7640, CFBH7644-7645, CFBH10940-10941, CFBH10944, CFBH10949
hh	*Thoropa miliaris*	Parque Nacional Caparaó	MG	20°30′21″S 41°54′55″W	1	—	—	MNRJ42089
	Outgroups							
	Thoropa megatympanum	Grão Mogol	MG	16°33′33.84″S 42°53′22.92″W	2	—	CFBH101998-10199	—
	Cycloramphus dubius	Rio do Ouro, Núcleo Pedro de Toledo, Parque Estadual da Serra do Mar	SP	24°11′17.40″S 47°2′46.39″W	1	—	MZUSP-A 135346	—